


The role of TRPC6 calcium channels and P2 purinergic receptors in podocyte mechanical and metabolic sensing

GEORGINA GYARMATI, ILDIKÓ TOMA, AUDREY IZUHARA,
JAMES L. BURFORD, URVI NIKHIL SHROFF, STELLA PAPADOURI,
SACHIN DEEPAK and JÁNOS PETI-PETERDI* 

Departments of Physiology and Neuroscience, and Medicine, Zilkha Neurogenetic Institute, University of Southern California, Los Angeles, CA 90033, USA

Received: October 15, 2021 • Accepted: November 22, 2021

© 2021 The Author(s)



ABSTRACT

Podocyte calcium (Ca^{2+}) signaling plays important roles in the (patho)physiology of the glomerular filtration barrier. Overactivation of podocyte transient receptor potential canonical (TRPC) channels including TRPC6 and purinergic signaling via P2 receptors that are known mechanosensors can increase podocyte intracellular Ca^{2+} levels ($[\text{Ca}^{2+}]_i$) and cause cell injury, proteinuria and glomerular disease including in diabetes. However, important mechanistic details of the trigger and activation of these pathways *in vivo* in the intact glomerular environment are lacking. Here we show direct visual evidence that podocytes can sense mechanical overload (increased glomerular capillary pressure) and metabolic alterations (increased plasma glucose) via TRPC6 and purinergic receptors including P2Y2. Multiphoton microscopy of podocyte $[\text{Ca}^{2+}]_i$ was performed *in vivo* using wild-type and TRPC6 or P2Y2 knockout (KO) mice expressing the calcium reporter GCaMP3/5 only in podocytes and *in vitro* using freshly dissected microperfused glomeruli. Single-nephron intra-glomerular capillary pressure elevations induced by obstructing the efferent arteriole lumen with laser-induced microthrombus *in vivo* and by a micropipette *in vitro* triggered >2-fold increases in podocyte $[\text{Ca}^{2+}]_i$. These responses were blocked in TRPC6 and P2Y2 KO mice. Acute elevations of plasma glucose caused >4-fold increases in podocyte $[\text{Ca}^{2+}]_i$ that were abolished by pharmacological inhibition of TRPC6 or P2 receptors using SAR7334 or suramin treatment, respectively. This study established the role of Ca^{2+} signaling via TRPC6 channels and P2 receptors in mechanical and metabolic sensing of podocytes *in vivo*, which are promising therapeutic targets in

* Corresponding author. Department of Physiology and Neuroscience, Zilkha Neurogenetic Institute, University of Southern California, 1501 San Pablo Street, ZNI 335, Los Angeles, CA 90033, USA. Tel.: +1 323 442 4337. E-mail: petipete@usc.edu

conditions with high intra-glomerular capillary pressure and plasma glucose, such as diabetic and hypertensive nephropathy.

KEYWORDS

podocyte, intravital imaging, multiphoton microscopy, TRPC6, P2Y2

INTRODUCTION

Glomerular podocytes in the kidney play major roles in the maintenance of the structure and function of the healthy glomerular filtration barrier (GFB) and in the development of glomerular pathologies [1]. Among the many molecular players of the podocyte slit diaphragm component of the GFB, transient receptor potential canonical (TRPC) channels including TRPC6 and purinergic P2 receptors including P2Y2 have been identified as key mechanisms in the regulation of podocyte intracellular Ca^{2+} levels ($[\text{Ca}^{2+}]_i$), development of cell injury, proteinuria and glomerular disease [2–8]. As part of their overall function, podocyte TRPC6 channels and P2 receptors (e.g. P2X4) have been initially suggested [9, 10] and subsequently confirmed experimentally using *in vitro* cell models [11–14] to act as molecular mechanosensors in the slit diaphragm that help maintain normal podocyte structure and function, but may also lead to disease development. While the mechanosensing hypothesis fits well with known functions of the podocyte slit diaphragm and with the molecular characteristics of TRPC6 and P2 receptors [15, 16], convincing *in vivo* studies have been lacking. In addition, a similarly untested metabolic sensory function of podocytes via TRPC6 and P2 receptors *in vivo* may add to the ability of podocytes to sense and respond to alterations in their local tissue environment [5, 17].

Due to the inaccessibility of podocytes and the 3D complexity of the GFB, podocytes have been traditionally difficult to study in their native environment *in vivo*. However, a new intravital imaging approach has been developed and applied recently to shed new light on podocyte functions including $[\text{Ca}^{2+}]_i$ signaling [2, 18, 19]. This direct visual approach employs intravital multiphoton microscopy (MPM) combined with new genetic mouse models for fluorescent podocyte labeling and tagging [2, 20, 21].

The present study aimed to test the mechanical and metabolic sensory function of podocytes *in vivo* by quantitatively visualizing the dynamic effects of high intra-glomerular capillary pressure as a solely mechanical stimulation, and increased plasma glucose levels as a metabolic stimulus on podocyte $[\text{Ca}^{2+}]_i$. In combination with genetic and pharmacological approaches, we also addressed the hypothesis that TRPC channels including TRPC6 and P2 purinoceptors including P2Y2 play important roles in podocyte mechano and metabolic sensing.

MATERIALS AND METHODS

Animals

Male and female, 4–8 weeks old wild-type (WT), TRPC6 and P2Y2 knockout (KO) C57BL/6J mice (Jackson Laboratory, Bar Harbor, ME) were used in all experiments. Pod-GCaMP3(G3) or



GCaMP5(G5) fluorescent reporter mice, which specifically express the intensely green and calcium-sensitive fluorescent protein GCaMP3 or GCaMP5, and the calcium insensitive red fluorescent dye tdTomato in podocytes (only with GCaMP5) were generated by crossing mice expressing Cre recombinase under the control of the podocin promoter [22] and GCaMP3flox or GCaMP5flox mice [23, 24]. Pod-G3/G5 fluorescent reporter mice were further backcrossed with TRPC6 [25] and P2Y2 KO mice [2, 26]. All mice were purchased from the Jackson laboratory. Some mice received intravenous glucose (4 g kg^{-1} in $50 \mu\text{L}$ PBS, NIST917C Sigma Aldrich, St. Louis, MO), or equimolar mannitol (PHR1007, Sigma Aldrich, St. Louis, MO) or the purinergic receptor blocker Suramin (50 mg kg^{-1} bolus followed by $150 \text{ mg kg}^{-1} \text{ h}^{-1}$ maintenance dose into the cannulated carotid artery, S2671, Sigma Aldrich, St. Louis, MO) injection, or the selective TRPC6 inhibitor SAR7334 (10 mg kg^{-1} in $50 \mu\text{L}$, 5,831 Tocris, Minneapolis, MN) via oral gavage. All animal protocols were approved by the Institutional Animal Care and Use Committee at the University of Southern California.

Tissue processing, histology and immunofluorescence

Immunofluorescence detection of proteins was performed as described previously [27]. Briefly, kidneys were perfused and fixed in 4% PFA for 2 h at room temperature, embedded in paraffin, and sectioned $8 \mu\text{m}$ thick. For immunofluorescence analysis of antibody stains, slides were washed in 1XPBS. For antigen retrieval, heat-induced epitope retrieval with Sodium Citrate buffer (pH 6.0) or Tris-EDTA (pH 9.0) was applied. To reduce non-specific binding, sections were blocked with normal serum (1:20). Primary and secondary antibodies were applied sequentially overnight at 4°C and 2 h at room temperature. Primary antibodies and dilutions were as follows: anti-TRPC6 antibody (1:100, ACC-120, Alomone Labs, Jerusalem, Israel), anti-P2Y2 antibody (1:100, APR-010, Alomone Labs, Jerusalem, Israel), anti-GFP antibody (GFP 1:200 Thermo Fisher Scientific, Waltham, MA). Alexa Fluor 488 and 594-conjugated secondary antibodies were purchased from Invitrogen (Waltham, MA). Slides were mounted by using DAPI-containing mounting media (VectaShield, Vector Laboratories Inc., Burlingame, CA). Sections were examined with Leica TCS SP8 (Leica Microsystems, Wetzlar, Germany) confocal/multiphoton laser scanning microscope systems as described previously [27, 28].

Intravital imaging using multiphoton microscopy (MPM)

Under continuous anesthesia (Isoflurane 1–2% inhalant via nose-cone), mice were placed on the stage of the inverted microscope with the exposed kidney mounted in a coverslip-bottomed chamber bathed in normal saline as described previously [29, 30]. Body temperature was maintained with a homeothermic blanket system (Harvard Apparatus). Alexa Fluor 594 or 680-conjugated albumin (Thermo Fisher, Waltham, MA) was administered iv. by retro-orbital injections to label the circulating plasma ($30 \mu\text{L}$ iv. bolus from $10 \mu\text{g mL}^{-1}$ stock solution). The images were acquired using a Leica SP8 DIVE multiphoton confocal fluorescence imaging system with a $40\times$ Leica water-immersion objective (numerical aperture (NA) 1.2) powered by a Chameleon Discovery laser at 860 nm or 960 nm (Coherent, Santa Clara, CA) and a DMI8 inverted microscope's external Leica 4Tune spectral hybrid detectors (emission at 510–530 nm for GCaMP3 and 5, at 580–640 nm for tdTomato and AF594, and at 680–740 for AF680) (Leica Microsystems, Heidelberg, Germany). The potential toxicity of laser excitation and fluorescence to the cells was minimized by using a low laser power and high scan speeds to keep total laser



exposure as minimal as possible. Fluorescence images were collected in volume and time series (xyt, 526 ms per frame) with the Leica LAS X imaging software and using the same instrument settings (laser power, offset, gain of both detector channels). The strong, positive, cell-specific signal (GCaMP3/5 – tdTomato fluorescence) and high-resolution MPM imaging allowed for easy identification of single podocyte cell bodies and processes. Acute intra-glomerular pressure elevation was induced by focusing the laser beam on a small focal point at the periphery of an endothelial cell in the efferent arteriole (EA) (approximately $1\text{-}\mu\text{m} \times 1\text{-}\mu\text{m}$ square-shaped ROI scan for 1 s at 20% laser power) to induce well-controlled and localized injury of a single endothelial cell resulting in microthrombi formation and obstruction of EA blood flow [31].

***In vitro* isolated and microperfused glomerulus**

Individual glomeruli with attached afferent (AA) and efferent (EA) arterioles were dissected freehand from freshly harvested kidneys of anesthetized mice and perfused *in vitro* using methods that were described before [32]. Briefly, the AA was cannulated and microperfused. Viability of each preparation was confirmed by the existence of small, spontaneous, and temporary vasoconstrictions in the AA. Dissection media were prepared from DMEM mixture F-12 (Sigma-Aldrich). Fetal bovine serum (Hyclone) was added at a final concentration of 3%. Arteriole perfusion and bath fluid was a modified Krebs-Ringer-HCO₃ buffer containing (in mM) 110 NaCl, 25 NaHCO₃, 0.96 NaH₂PO₄, 0.24 Na₂HPO₄, 5 KCl, 1.2 MgSO₄, 2 CaCl₂, 5.5 D-glucose, and 100 μM L-arginine. The pH of the solutions was adjusted to 7.4. Each preparation was transferred to a thermoregulated Lucite chamber mounted on an inverted microscope (Leica TCS SP8, 63 \times glycerol immersion objective). The preparation was kept in the dissection solution, and also, temperature was kept at 4 °C until cannulation of the arteriole was completed and then gradually raised to 37 °C for the remainder of the experiment. The bath was continuously exchanged (1 mL min^{-1}) and oxygenized (95% O₂–5% CO₂) throughout the whole experiment. Elevations in glomerular capillary pressure was triggered by obstructing the EA lumen by pressing down the EA with a glass micropipette with the help of a micromanipulator (MP-225; Sutter Instrument, Novato, CA), while maintaining AA perfusion pressure (50 mmHg) constant as described before [32].

Quantification of GCaMP3/5 fluorescence intensity

An optical section including a glomerulus was selected and time (xyt) series with 1 frame per 526 ms were recorded for 2–15 min to measure $[\text{Ca}^{2+}]_i$ dynamics. The strong, positive signal (GCaMP3 and GCaMP5/tdTomato fluorescence) and high-resolution MPM imaging allowed for easy identification of single podocytes. For the quantification of changes in mean GCaMP3 and 5 fluorescence intensity, ROIs were drawn closely over the total cell body of single podocytes or over the entire glomerulus and the changes in GCaMP3/5 F_{max}/F_0 (green channel; fluorescence intensity expressed as a ratio relative to baseline) were measured after the experiment in the defined ROI using the Quantify package of LAS X software (3.6.0.20104; Leica-Microsystems) as described before [2].

Statistical methods

Data are expressed as average \pm SEM and were analyzed using Student's *t*-tests (between two groups), or ANOVA (for multiple groups) with post-hoc comparison by Bonferroni test.



$P < 0.05$ was considered significant. Statistical analyses were performed using GraphPad Prism 9.0.1 (GraphPad Software, Inc.).

RESULTS

Mechanosensation by podocytes *in vivo* and *in vitro*

These studies performed time-lapse high resolution multiphoton microscopy (MPM) of the intact living kidney of WT, and TRPC6 or P2Y2 knockout (KO) Pod-GCaMP3 or Pod-GCaMP5 mice to directly and quantitatively visualize changes in podocyte $[Ca^{2+}]_i$ in the local glomerular tissue environment *in vivo*. TRPC6 and P2Y2 deficiency was confirmed by immunohistochemistry in TRPC6 and P2Y2 KO mice, respectively, compared to their WT littermates (Fig. 1A). All mice featured the genetically expressed Ca^{2+} -sensitive reporter, either GCaMP3 alone or GCaMP5 (both green) together with the Ca^{2+} -insensitive tdTomato (red) specifically in podocytes, driven by the podocin (Pod) promoter in a Cre-lox system (Fig. 1B). In this study, glomeruli of cortical nephrons approximately 150 μm under the kidney surface were visualized. Figure 1B demonstrates that a great number (>50) of superficial glomeruli were available for MPM imaging. On close-up images, individual GCaMP expressing podocytes with their cell processes were visible in great detail (Fig. 1B).

We first used MPM imaging of Pod-GCaMP3 mice *in vivo* and devised a maneuver to generate glomerular capillary pressure elevations acutely in single nephrons by obstructing the blood flow of the efferent arteriole (glomerular outflow) with a laser-induced microthrombus in the vessel lumen (Fig. 2A, Supplement Movie 1 available at <https://figshare.com/s/9d9073bc01b179742459>). The observed, approximately 10% increase in glomerular capillary and tuft diameter in response to obstructing the efferent arteriole lumen indicated successfully elevated glomerular capillary pressure (Fig. 2A). Importantly, this maneuver triggered >2-fold increases in $[Ca^{2+}]_i$ in several podocytes as compared to baseline, based on normalized changes in single cell GCaMP3 fluorescence intensity as an indicator for podocyte $[Ca^{2+}]_i$ changes (Fig. 2B). Capillary pressure-induced podocyte $[Ca^{2+}]_i$ elevations were blocked in TRPC6 (0.84 ± 0.08 -fold) and P2Y2 KO mice (0.86 ± 0.05 -fold) compared to WT (2.09 ± 0.18 -fold, $P < 0.05$, 2 glomeruli/mouse from $n = 5$ mice in each group) (Fig. 2B). In addition, the presence and magnitude of these podocyte $[Ca^{2+}]_i$ responses were confirmed using the Pod-GCaMP5/tdTomato mouse model. The same capillary pressure elevation maneuver triggered similar, 2.23 ± 0.17 -fold podocyte $[Ca^{2+}]_i$ elevations ($n = 6$, data not shown). Simultaneous increases in $[Ca^{2+}]_i$ in numerous distant podocytes indicated the presence of primary responses to pressure elevation, while some podocytes triggered cell-to-cell propagating $[Ca^{2+}]_i$ waves (Fig. 2A and C, Supplement Movie 1). In response to this maneuver, albumin leakage through the GFB developed as evident by the appearance of labeled albumin in the Bowman's space. Interestingly, GFB albumin leakage preceded podocyte $[Ca^{2+}]_i$ elevations (Fig. 2C, Supplement Movie 1).

To confirm capillary pressure-induced elevations in podocyte $[Ca^{2+}]_i$ in a model that is free of potential non-specific influences by alterations in systemic or the local microthrombotic environment, we next used freshly dissected and microperfused glomeruli *in vitro* from the same mouse models (Fig. 3A–D, Supplement Movie 2, available at <https://figshare.com/s/9d9073bc01b179742459z>). In this model, glomerular capillary pressure elevations were induced by obstructing the efferent arteriole outflow with a micropipette while afferent arteriole



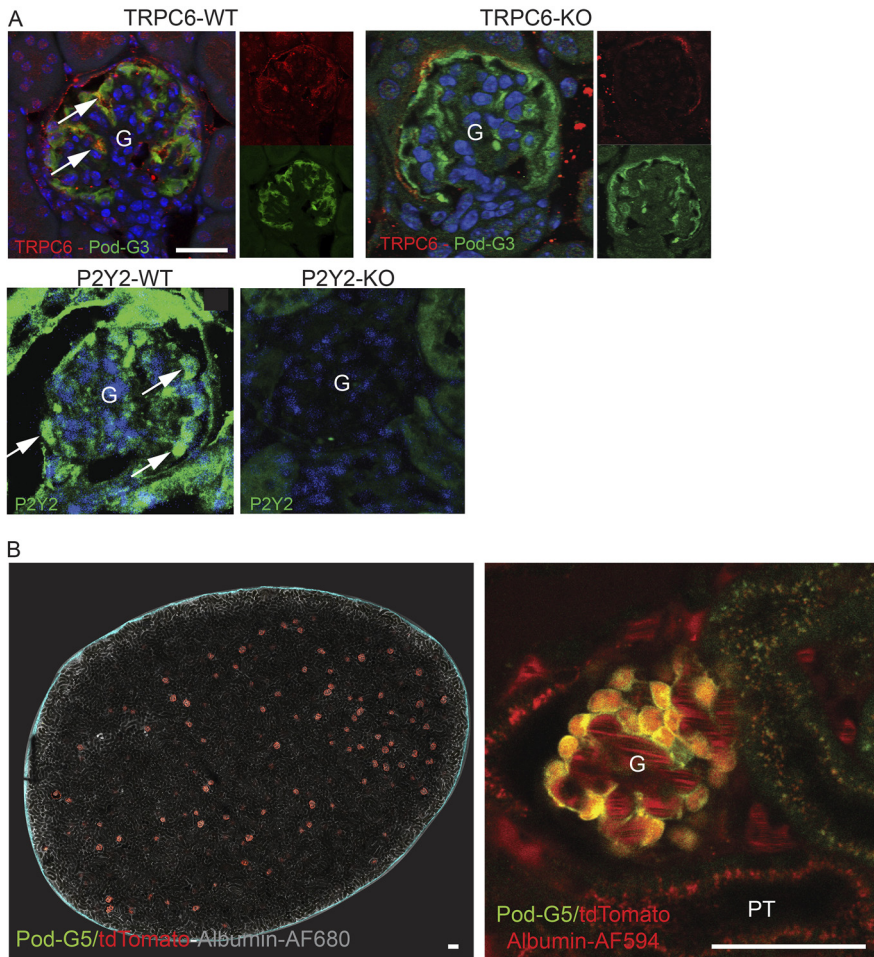


Fig. 1. Molecular and intravital MPM imaging features of the applied wild-type (WT) and TRPC6 or P2Y2 KO Pod-GCaMP3/5 mouse models.

(A) Immunofluorescence localization of TRPC6 (red) with GCaMP3 (G3) co-labeling (green), or P2Y2 (green) in wild type (WT), TRPC6 KO or P2Y2 KO mouse kidney tissue sections as indicated. Overlay of green and/or red channels with the nuclear stain DAPI (blue) is shown. For TRPC6 WT and KO tissues, individual red and green channels are included separately in insets. Note the strong TRPC6 (co-localized with Pod-G3) or P2Y2 labeling in podocytes (arrows) in WT, but the absence of TRPC6 or P2Y2 labeling in TRPC6 KO or P2Y2 KO mouse kidney sections, respectively.

(B) Representative intravital MPM images of the overview of the entire renal cortex area that is available for MPM imaging (left, tile-scan) or a single glomerulus with high-magnification (right, single xy frame) from a WT Pod-GCaMP5 (G5, green)/tdTomato (red) mouse. The fibrous renal capsule was visualized with second harmonic generation (SHG, cyan). The plasma was labeled using Albumin-Alexa Fluor 680 (grey) or Albumin-Alexa Fluor 594 (red). Note the high number of renal cortical glomeruli (left panel) available for MPM imaging and the clear view of individual podocytes co-expressing G5 and tdTomato (yellow, right panel). G: glomerulus. Scale bar is 20 μm for panel A and 100 μm for panel B



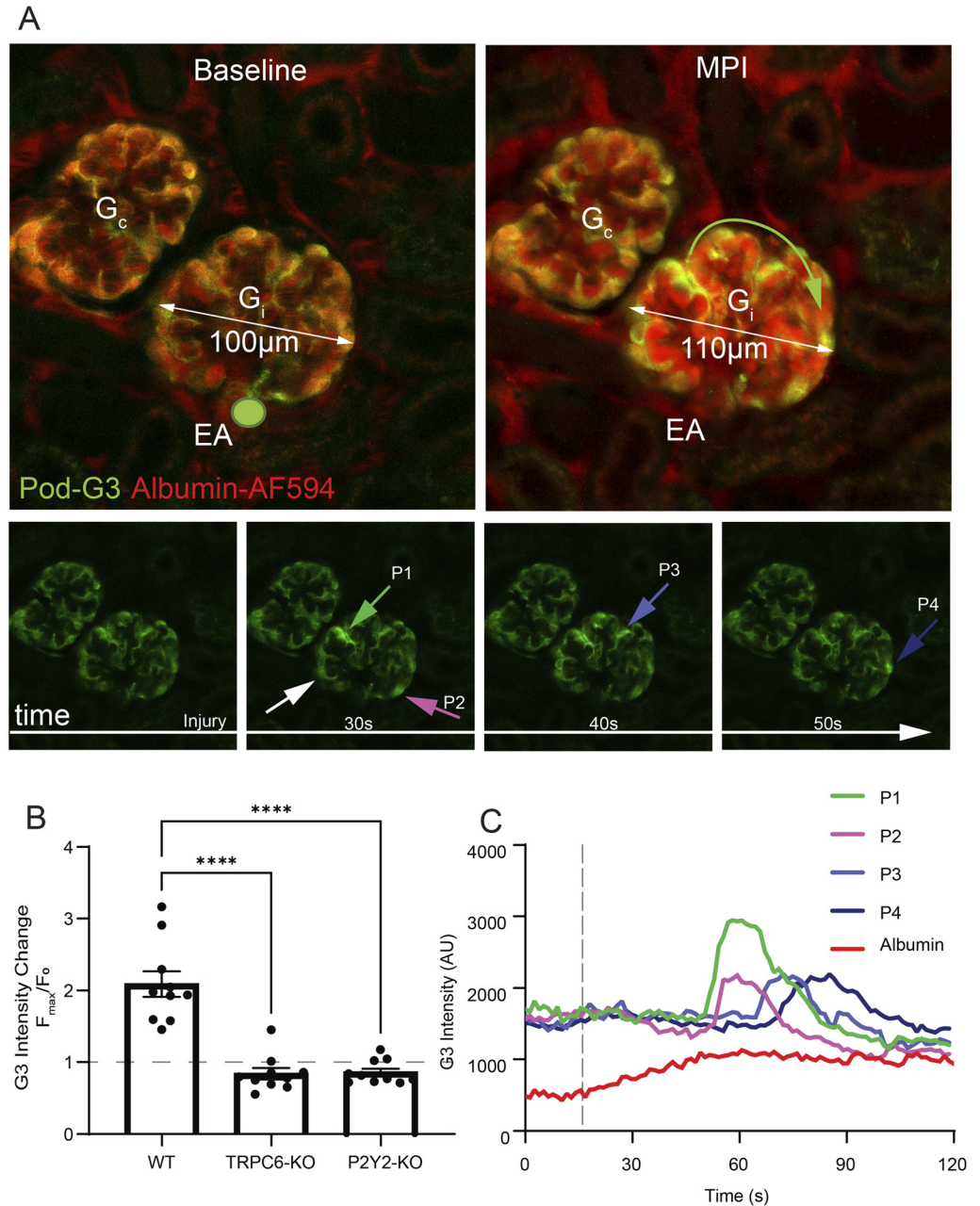


Fig. 2. Podocyte $[Ca^{2+}]_i$ responses to mechanical overload *in vivo*.

(A) Representative single-frame xy image at baseline (left) and maximum projection image (MPI) of a 40 second time-lapse after injury (right) of two glomeruli in WT Pod-GCaMP3 mice. A short pulse of a laser



perfusion was maintained constant. This maneuver caused on average an 8–10% increase in glomerular capillary and tuft diameter, which was uniform in all experimental groups (Fig. 3D). In response to glomerular capillary pressure elevations, podocyte GCaMP3 fluorescence intensity significantly increased in several but not all podocytes in preparations from WT mice (2.20 ± 0.04 -fold) (Fig. 3A–C). Podocyte $[Ca^{2+}]_i$ responses were diminished in preparations from TRPC6 KO (1.04 ± 0.01 -fold) and P2Y2 KO mice (1.09 ± 0.01 -fold, $P < 0.05$, $n = 10$ in each group) (Fig. 3C, Supplemental Video 2).

Metabolic (glucose) sensing by podocytes *in vivo*

To test whether podocytes can sense metabolic signals via $[Ca^{2+}]_i$ *in vivo*, specifically increased plasma glucose as seen in diabetes, Pod-GCaMP5/tdTomato mice were subjected to acute plasma glucose loading that resulted in plasma glucose levels uniformly at 500 ± 50 mg dL⁻¹. To control for elevated plasma osmolality, equimolar mannitol infusions were performed. Acute hyperglycemia caused elevations in $[Ca^{2+}]_i$ in all podocytes in untreated WT mice with a biphasic response, a robust peak (4.20 ± 0.16 -fold elevation) followed by a prolonged plateau (1.53 ± 0.09 -fold elevation). In contrast, hyperglycemia-induced podocyte $[Ca^{2+}]_i$ responses were diminished in mice pre-treated with the selective TRPC6 inhibitor SAR7334 (1.37 ± 0.19 and 1.13 ± 0.08 -fold increases in peak and plateau, respectively) or with the purinergic P2 receptor blocker suramin (2.44 ± 0.36 and 1.17 ± 0.08 -fold increases in peak and plateau, respectively). Compared to high glucose, equimolar mannitol plasma loading did not produce elevations in podocyte $[Ca^{2+}]_i$ in untreated WT mice (1.16 ± 0.08 and 0.98 ± 0.04 -fold increases in peak and plateau, respectively).

DISCUSSION

This study applied intravital MPM imaging combined with genetic and pharmacological inhibition of TRPC6 calcium channels and P2 purinergic receptors to uncover novel mechanistic

beam focused on a small focal point of the efferent arteriole (EA) endothelium of one glomerulus (G_i , denoted by green circle) caused localized endothelial injury and formation of a microthrombus in the lumen of the EA. The other adjacent glomerulus (G_c) was left intact and served as control. Note the glomerular tuft distension indicating capillary pressure elevation, increased podocyte $[Ca^{2+}]_i$ (increase in GCaMP3 fluorescent intensity-bright green, including a cell-to-cell propagating podocyte $[Ca^{2+}]_i$ wave indicated by a green arrow), and albumin leakage into the Bowman's space (red around the glomerular capillaries) only in the injured glomerulus (G_i) (a time-lapse recording of the same preparation is shown in Supplemental Movie 1).

GCaMP3 images are included (bottom) that illustrate the changes in podocyte $[Ca^{2+}]_i$ in response to glomerular capillary pressure elevations over time (baseline at time of injury, and 30–40–50 s later). Note the high $[Ca^{2+}]_i$ in distant podocytes appearing simultaneously (P_1 – P_2), or with a delay in a cell-to-cell propagating podocyte $[Ca^{2+}]_i$ wave (P_1 – P_3 – P_4).

(B) Summary of podocyte $[Ca^{2+}]_i$ responses (normalized to baseline, dashed line) to mechanical overload in WT, TRPC6-KO, and P2Y2-KO animals. Data represent mean \pm SEM, ****: $P < 0.0001$, 2 glomeruli/mouse from $n = 5$ mice in each group).

(C) Representative recordings of single-cell podocyte $[Ca^{2+}]_i$ responses over time illustrating the dynamics of $[Ca^{2+}]_i$ changes in four different podocytes during capillary pressure elevation (time of microthrombus formation indicated by vertical line). Different colors represent P_1 – P_4 single podocytes matching those shown in panel A (bottom). Time-course of albumin appearing in the Bowman's space is indicated by red line



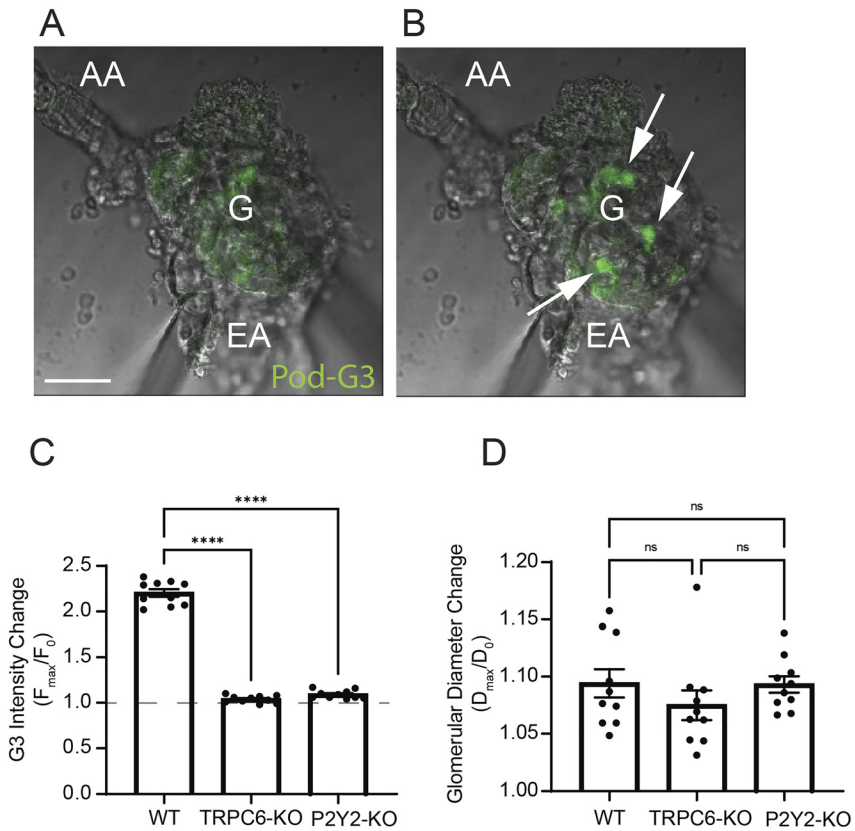


Fig. 3. Podocyte $[Ca^{2+}]_i$ responses to mechanical overload in microperfused glomeruli *in vitro*. (A-B) Representative images of a freshly dissected and *in vitro* microperfused glomerulus (G) from a WT Pod-GCaMP3 mouse kidney at baseline (A) and after obstructing the efferent arteriole (EA) lumen by a micropipette (B, mechanical overload). Note the increased podocyte GCaMP3 fluorescence (green, arrows) after glomerular capillary pressure elevation (B) compared to baseline (A). DIC overlay is shown with GCaMP3 fluorescence. Afferent arteriole (AA) perfusion was kept constant. Bar is 20 μ m. The same preparation is shown in Supplement Movie 2. (C) Summary of the changes in podocyte $[Ca^{2+}]_i$ (GCaMP3 fluorescence normalized to baseline (dashed line), F_{max}/F_0) in response to mechanical overload in preparations from WT, TRPC6-KO, and P2Y2-KO animals. (D) Changes in glomerular diameter in response to mechanical overload in each group. Data represent mean \pm SEM, ns: not significant, ****: $P < 0.0001$, $n = 10$ in each group.

insights of podocyte mechanical and metabolic sensing. Direct *in vivo* visual evidence was presented to support podocyte mechanosensitivity, specifically the ability of podocytes to directly detect and respond to elevations in intra-glomerular capillary pressure via $[Ca^{2+}]_i$ signaling that involved TRPC6 calcium channels and P2Y2 purinergic receptors. In addition, podocytes showed extremely high sensitivity to alterations in the systemic metabolic



environment, specifically increased plasma glucose levels that triggered even higher $[Ca^{2+}]_i$ elevations that similarly involved TRPC6 calcium channels and P2 purinergic receptors. These key findings provide further confirmation, at the *in vivo* level, that podocyte $[Ca^{2+}]_i$ signaling via TRPC6 calcium channels and P2 receptors play important pathological roles in podocyte and glomerular injury and disease.

Intravital MPM imaging performed in the present study used podocyte-specific expression of genetically encoded $[Ca^{2+}]_i$ reporters GCaMP3 as in earlier studies [2, 18, 19], as well as GCaMP5 which is an improved, more $[Ca^{2+}]_i$ sensitive version [24]. In fact, detailed micro-anatomical features of podocytes including cell processes were clearly observed with MPM imaging of Pod-GCaMP5/*tdTomato* mice (Fig. 1B). In addition, Fig. 1B confirmed the presence of a great number of superficial glomeruli in the mouse renal cortex and their availability for performing quantitative imaging measurements such as in the present study.

The key pathogenic roles of $[Ca^{2+}]_i$ elevations mediated by TRPC calcium channels including TRPC6 [3, 6, 8, 17] and TRPC5 [33], and purinergic receptors including P2Y2, P2X4 and others [2, 5, 13] in podocyte injury and glomerular pathologies have been well documented. Specifically, earlier fluorescence imaging studies have used cell culture or dissected glomeruli and reported podocyte $[Ca^{2+}]_i$ responses to a variety of stimuli *in vitro* including mechanical load and diabetic conditions [4, 13, 17, 32–34]. Following initial proposals that TRPC6 in podocytes may play a mechanosensory role [9, 10], Dryer and co-workers showed experimentally that TRPC6 channels in cultured podocytes can be activated by many different mechanical stimuli [11, 12, 14]. Forst et al. identified the role of P2X4 in podocyte mechanosensing by measuring the effects of hypoosmolality and pipette pressure rather than directly physiologically relevant stimuli on $[Ca^{2+}]_i$ responses of cultured podocytes [13]. Only a few studies measured podocyte $[Ca^{2+}]_i$ responses *in vivo* in the intact kidney [2, 18, 19], however none of these addressed the effects of mechanical, hemodynamic or metabolic stimuli. The present study applied physiologically and pathologically relevant conditions and demonstrated increased glomerular capillary pressure (Figs 2–3) and plasma glucose-induced elevations in podocyte $[Ca^{2+}]_i$ *in vivo* (Fig. 4). These findings are consistent with the mechanosensing and metabolic sensing functions and their roles in the physiological maintenance or pathological changes of these important glomerular cell types. Subsequent experiments confirmed the mechanistic role of TRPC6 calcium channels and P2 purinoceptors including P2Y2 in these podocyte functions (Figs 2–4).

Transient elevations in podocyte $[Ca^{2+}]_i$ in response to either acute mechanical load or high plasma glucose as demonstrated in the present experiments may be relevant and important in the physiological context. By strengthening the actin-cytoskeleton and cell adhesion, these sensory mechanisms may help podocytes counteract increased glomerular mechanical strain during blood pressure fluctuations and postprandial hyperfiltration, maintain GFB permeability and functions, and prevent podocyte detachment. However, sustained mechanical and metabolic stimuli and elevations in podocyte $[Ca^{2+}]_i$ via gain-of-function of TRPC6 ion channels and/or P2 purinergic receptors during disease conditions play well-known major roles in podocyte injury, foot process effacement and glomerular pathology development [5, 9, 10, 13, 18]. The presently observed features of podocyte mechanosensing including heterogeneity (Figs 2–3), cell-to-cell propagation (Fig. 2A and C, Supplement Movie 1), TRPC6 channel and P2 receptor dependence of $[Ca^{2+}]_i$ responses (Figs 2–4) are consistent with earlier reports [2, 4, 5, 13, 18]. Interestingly, the present studies observed high capillary pressure-induced $[Ca^{2+}]_i$ increases in several but not all podocytes (Figs 2–3). This finding is consistent with the heterogeneity of



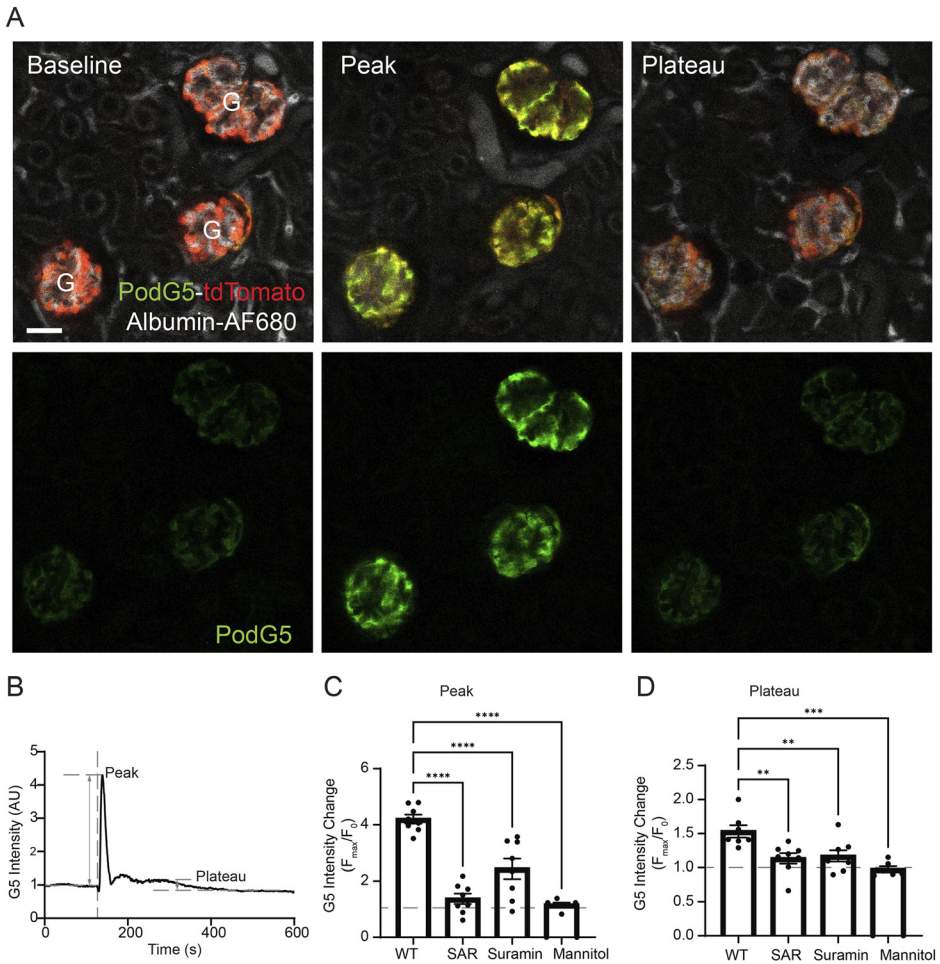


Fig. 4. Podocyte $[Ca^{2+}]_i$ responses to increased plasma glucose *in vivo*.

(A) Representative intravital MPM images of the same glomeruli from WT Pod-GCaMP5(G5)/tdTomato mice at baseline (left), and at the peak (center) and plateau phase (right) of acute hyperglycemia-induced elevations in podocyte $[Ca^{2+}]_i$. Overlay of calcium-sensitive GCaMP5 (PodG5, green), calcium-insensitive tdTomato (red), and plasma marker (albumin-Alexa Fluor 680) signals (top row), or GCaMP5 (green) signals shown separately (bottom row). Note the robust elevations in GCaMP5 signal at peak compared to plateau or baseline.

(B) Representative recording of podocyte $[Ca^{2+}]_i$ in response to acute hyperglycemia, with peak and plateau phases indicated.

(C-D) Summary of the peak (C) or plateau (D) phase of acute hyperglycemia-induced podocyte $[Ca^{2+}]_i$ elevations (normalized to baseline, dashed line) in untreated WT mice, and after pre-treatment with the selective TRPC6 inhibitor SAR7334, or with the purinergic P2 receptor blocker Suramin, or with equimolar Mannitol. Data represent mean \pm SEM, **: $P < 0.01$, ***: $P < 0.0001$, 2 glomeruli/mouse from $n = 4$ mice in each group.



TRPC6 expression between individual podocytes including in the same glomerulus, but it could be explained also, at least partially, by the presence of different mechanical strain in different areas of glomerular capillaries (e.g. in the recently described afferent/efferent arteriole chamber [35] vs. inside a single capillary segment). Similarly heterogenous, TRPC6-dependent $[Ca^{2+}]_i$ responses of podocytes to angiotensin II have been reported in a recent study [18]. The cell-to-cell propagating $[Ca^{2+}]_i$ wave during glomerular capillary pressure elevation (Fig. 2A and C) is consistent with the previously described phenomenon of secondary podocyte injury [36, 37], and with the P2 receptor-mediated podocyte $[Ca^{2+}]_i$ wave that was demonstrated in our previous intravital MPM imaging study [2]. TRPC6 channel and P2 receptor dependence of podocyte mechano and metabolic sensing found in the present work (Figs 2–4) is in agreement with most but not all earlier works by others and further substantiates the important role of these molecular pathways in podocyte function [3–5, 18, 34]. The lack of TRPC6 dependence of podocyte mechanosensory function found in an earlier study [13] may be explained by the non-physiological stimuli and cell culture model applied in that study compared to the *in vivo* and (patho)physiological approaches used in the present study. It should be noted that the presently applied pharmacological inhibitors of TRPC channels (SAR7334) and purinergic P2 receptors (suramin) (Fig. 4) are non-selective antagonists of these molecular $[Ca^{2+}]_i$ signaling pathways, although SAR7334 is fairly specific for TRPC6 [4, 38]. Therefore, we cannot exclude the possibility of other TRPC channels and/or P2 receptors contributing to podocyte mechano and metabolic sensing. While a few studies implicated the role of podocyte P2X receptors [5, 13], P2Y metabotropic purinoceptors were shown as the main purinergic Ca^{2+} pathway in podocytes in several prior reports [2, 7, 39] and in the present study (Figs 2–3). The finding that podocytes may be more sensitive to metabolic (high glucose, Fig. 4) compared to mechanical (high capillary pressure, Figs 2–3) stimuli is an interesting new insight relevant to diabetic vs hypertensive kidney diseases and requires further exploration in future studies.

Interestingly, we found that GFB albumin leakage preceded podocyte $[Ca^{2+}]_i$ elevations (Fig. 2) suggesting that hemodynamic changes rather than elevations in podocyte $[Ca^{2+}]_i$ played causative roles in albumin leakage. The role of glomerular endothelial injury and microthrombi in podocyte detachment and albumin leakage via hemodynamic and mechanical forces has been reviewed recently by our group [40]. Further support for the role of hemodynamics vs. podocyte $[Ca^{2+}]_i$ per se was provided by acute manipulations of podocyte $[Ca^{2+}]_i$ using intravital MPM imaging of a DREADD mouse model that found no immediate effects on podocyte or glomerular functions [19].

In summary, the present study directly demonstrated the role of Ca^{2+} signaling via TRPC6 channels and P2 receptors in the mechanical and metabolic sensory capacity of podocytes *in vivo*. These cell and molecular mechanisms are promising therapeutic targets in conditions with high intra-glomerular capillary pressure and altered systemic metabolism, such as diabetic and hypertensive nephropathy for the prevention of kidney diseases.

ACKNOWLEDGMENTS

This work was supported in part by US National Institutes of Health grants DK100944 to J.P.-P. Fluorescence imaging was performed at the USC Multi-Photon Microscopy Core funded by the National Institute of Health grant S10OD021833.



SUPPLEMENTARY MATERIAL

Supplementary data to this article can be found online at <https://doi.org/10.1556/2060.2021.00205>.

REFERENCES

1. Pavenstädt H, Kriz W, Kretzler M. Cell biology of the glomerular podocyte. *Physiol Rev* 2003; 83(1): 253–307.
2. Burford JL, Villanueva K, Lam L, Riquier-Brison A, Hackl MJ, Pippin J, et al. Intravital imaging of podocyte calcium in glomerular injury and disease. *J Clin Invest* 2014; 124(5): 2050–8.
3. Eckel J, Lavin PJ, Finch EA, Mukerji N, Burch J, Gbadegesin R, et al. TRPC6 enhances angiotensin II-induced albuminuria. *J Am Soc Nephrol* 2011; 22(3): 526–35.
4. Ilatovskaya DV, Palygin O, Levchenko V, Endres BT, Staruschenko A. The role of angiotensin II in glomerular volume dynamics and podocyte calcium handling. *Sci Rep* 2017; 7(1): 299.
5. Palygin O, Klemens CA, Isaeva E, Levchenko V, Spires DR, Dissanayake LV, et al. Characterization of purinergic receptor 2 signaling in podocytes from diabetic kidneys. *iScience* 2021; 24(6): 102528.
6. Reiser J, Polu KR, Möller CC, Kenlan P, Altintas MM, Wei C, et al. TRPC6 is a glomerular slit diaphragm-associated channel required for normal renal function. *Nat Genet* 2005; 37(7): 739–44.
7. Roshanravan H, Dryer SE. ATP acting through P2Y receptors causes activation of podocyte TRPC6 channels: role of podocin and reactive oxygen species. *Am J Physiol Renal Physiol* 2014; 306(9): F1088–97.
8. Winn MP, Conlon PJ, Lynn KL, Farrington MK, Creazzo T, Hawkins AF, et al. A mutation in the TRPC6 cation channel causes familial focal segmental glomerulosclerosis. *Science* 2005; 308(5729): 1801–4.
9. Huber TB, Schermer B, Benzing T. Podocin organizes ion channel-lipid supercomplexes: implications for mechanosensation at the slit diaphragm. *Nephron Exp Nephrol* 2007; 106(2): e27–31.
10. Möller CC, Flesche J, Reiser J. Sensitizing the slit diaphragm with TRPC6 ion channels. *J Am Soc Nephrol* 2009; 20(5): 950–3.
11. Anderson M, Kim EY, Hagmann H, Benzing T, Dryer SE. Opposing effects of podocin on the gating of podocyte TRPC6 channels evoked by membrane stretch or diacylglycerol. *Am J Physiol Cell Physiol* 2013; 305(3): C276–89.
12. Dryer SE, Roshanravan H, Kim EY. TRPC channels: regulation, dysregulation and contributions to chronic kidney disease. *Biochim Biophys Acta Mol Basis Dis* 2019; 1865(6): 1041–66.
13. Forst AL, Olteanu VS, Mollet G, Wlodkowski T, Schaefer F, Dietrich A, et al. Podocyte purinergic P2X4 channels are mechanotransducers that mediate cytoskeletal disorganization. *J Am Soc Nephrol* 2016; 27(3): 848–62.
14. Kim EY, Roshanravan H, Dryer SE. Changes in podocyte TRPC channels evoked by plasma and sera from patients with recurrent FSGS and by putative glomerular permeability factors. *Biochim Biophys Acta Mol Basis Dis* 2017; 1863(9): 2342–54.
15. Welsh DG, Morielli AD, Nelson MT, Brayden JE. Transient receptor potential channels regulate myogenic tone of resistance arteries. *Circ Res* 2002; 90(3): 248–50.
16. Kong Q, Quan Y, Tian G, Zhou J, Liu X. Purinergic P2 receptors: novel mediators of mechanotransduction. *Front Pharmacol* 2021; 12: 671809.



17. Ilatovskaya DV, Blass G, Palygin O, Levchenko V, Pavlov TS, Grzybowski MN, et al. A NOX4/TRPC6 pathway in podocyte calcium regulation and renal damage in diabetic kidney disease. *J Am Soc Nephrol* 2018; 29(7): 1917–27.
18. Binz-Lotter J, Jüngst C, Rinschen MM, Koehler S, Zentis P, Schauss A, et al. Injured podocytes are sensitized to angiotensin II-induced calcium signaling. *J Am Soc Nephrol* 2020; 31(3): 532–42.
19. Koehler S, Brähler S, Kuczowski A, Binz J, Hackl MJ, Hagmann H, et al. Single and transient Ca(2+) peaks in podocytes do not induce changes in glomerular filtration and perfusion. *Sci Rep* 2016; 6: 35400.
20. Hackl MJ, Burford JL, Villanueva K, Lam L, Suszták K, Schermer B, et al. Tracking the fate of glomerular epithelial cells in vivo using serial multiphoton imaging in new mouse models with fluorescent lineage tags. *Nat Med* 2013; 19(12): 1661–6.
21. Peti-Peterdi J, Kidokoro K, Riquier-Brison A. Novel in vivo techniques to visualize kidney anatomy and function. *Kidney Int* 2015; 88(1): 44–51.
22. Moeller MJ, Sanden SK, Soofi A, Wiggins RC, Holzman LB. Podocyte-specific expression of cre recombinase in transgenic mice. *Genesis* 2003; 35(1): 39–42.
23. Zariwala HA, Borghuis BG, Hoogland TM, Madisen L, Tian L, De Zeeuw CI, et al. A Cre-dependent GCaMP3 reporter mouse for neuronal imaging in vivo. *J Neurosci* 2012; 32(9): 3131–41.
24. Gee JM, Smith NA, Fernandez FR, Economo MN, Brunert D, Rothermel M, et al. Imaging activity in neurons and glia with a Polr2a-based and cre-dependent GCaMP5G-IRES-tdTomato reporter mouse. *Neuron* 2014; 83(5): 1058–72.
25. Dietrich A, Mederos YSM, Gollasch M, Gross V, Storch U, Dubrovskaya G, et al. Increased vascular smooth muscle contractility in TRPC6^{-/-} mice. *Mol Cell Biol* 2005; 25(16): 6980–9.
26. Homolya L, Watt WC, Lazarowski ER, Koller BH, Boucher RC. Nucleotide-regulated calcium signaling in lung fibroblasts and epithelial cells from normal and P2Y(2) receptor (-/-) mice. *J Biol Chem* 1999; 274(37): 26454–60.
27. Riquier-Brison ADM, Sipos A, Prókai Á, Vargas SL, Toma L, Meer EJ, et al. The macula densa prorenin receptor is essential in renin release and blood pressure control. *Am J Physiol Renal Physiol* 2018; 315(3): F521–f34.
28. Gyarmati G, Shroff UN, Riquier-Brison A, Kriz W, Kaissling B, Neal CR, et al. A new view of macula densa cell microanatomy. *Am J Physiol Renal Physiol* 2021; 320(3): F492–f504.
29. Kang JJ, Toma I, Sipos A, McCulloch F, Peti-Peterdi J. Quantitative imaging of basic functions in renal (patho)physiology. *Am J Physiol Renal Physiol* 2006; 291(2): F495–502.
30. Shroff UN, Schiessl IM, Gyarmati G, Riquier-Brison A, Peti-Peterdi J. Novel fluorescence techniques to quantitate renal cell biology. *Methods Cell Biol* 2019; 154: 85–107.
31. Peti-Peterdi J, Sipos A. A high-powered view of the filtration barrier. *J Am Soc Nephrol* 2010; 21(11): 1835–41.
32. Peti-Peterdi J. Calcium wave of tubuloglomerular feedback. *Am J Physiol Renal Physiol* 2006; 291(2): F473–80.
33. Schaldecker T, Kim S, Tarabanis C, Tian D, Hakrrouch S, Castonguay P, et al. Inhibition of the TRPC5 ion channel protects the kidney filter. *J Clin Invest* 2013; 123(12): 5298–309.
34. Spires D, Ilatovskaya DV, Levchenko V, North PE, Geurts AM, Palygin O, et al. Protective role of Trpc6 knockout in the progression of diabetic kidney disease. *Am J Physiol Renal Physiol* 2018; 315(4): F1091–f7.
35. Neal CR, Arkill KP, Bell JS, Betteridge KB, Bates DO, Winlove CP, et al. Novel hemodynamic structures in the human glomerulus. *Am J Physiol Renal Physiol* 2018; 315(5): F1370–f84.
36. Matsusaka T, Sandgren E, Shintani A, Kon V, Pastan I, Fogo AB, et al. Podocyte injury damages other podocytes. *J Am Soc Nephrol* 2011; 22(7): 1275–85.



37. Okabe M, Yamamoto K, Miyazaki Y, Motojima M, Ohtsuka M, Pastan I, et al. Indirect podocyte injury manifested in a partial podocytectomy mouse model. *Am J Physiol Renal Physiol* 2021; 320(5): F922–f33.
38. Maier T, Follmann M, Hessler G, Kleemann HW, Hachtel S, Fuchs B, et al. Discovery and pharmacological characterization of a novel potent inhibitor of diacylglycerol-sensitive TRPC cation channels. *Br J Pharmacol* 2015; 172(14): 3650–60.
39. Ilatovskaya DV, Palygin O, Levchenko V, Staruschenko A. Pharmacological characterization of the P2 receptors profile in the podocytes of the freshly isolated rat glomeruli. *Am J Physiol Cell Physiol* 2013; 305(10): C1050–9.
40. Gyarmati G, Jacob CO, Peti-Peterdi J. New endothelial mechanisms in glomerular (Patho)biology and proteinuria development captured by intravital multiphoton imaging. *Front Med (Lausanne)* 2021; 8: 765356.

Open Access. This is an open-access article distributed under the terms of the Creative Commons Attribution-NonCommercial 4.0 International License (<https://creativecommons.org/licenses/by-nc/4.0/>), which permits unrestricted use, distribution, and reproduction in any medium for non-commercial purposes, provided the original author and source are credited, a link to the CC License is provided, and changes – if any – are indicated.

